Computers, Materials & Continua CMC, vol.64, no.3, pp. 1587-1599, 2020

Gain-Enhanced Metamaterial Based Antenna for 5G Communication Standards

Daniyal Ali Sehrai[1], Fazal Muhammad[1], Saad Hassan Kiani[1], Ziaul Haq Abbas[2], Muhammad Tufail[3] and Sunghwan Kim[4, *]

Abstract: Metamaterial surfaces play a vital role to achieve the surface waves suppression and in-phase reflection, in order to improve the antenna performance. In this paper, the performance comparison of a fifth generation (5G) antenna design is analyzed and compared with a metamaterial-based antenna for 5G communication system applications. Metamaterial surface is utilized as a reflector due to its in-phase reflection characteristic and high-impedance nature to improve the gain of an antenna. As conventional conducting ground plane does not give enough surface waves suppression which affects the antenna performance in terms of efficiency and gain etc. These factors are well considered in this work and improved by using the metamaterial surface. The radiating element of the proposed metamaterial based antenna is made up of copper material which is backed by the substrate, i.e., Rogers-4003 with a standard thickness, loss tangent and a relative permittivity of 1.524 mm, 0.0027 and 3.55, correspondingly. The proposed antenna with and without metamaterial surface operates at the central frequency of 3.32 GHz and 3.60 GHz, correspondingly. The traditional antenna yields a boresight gain of 2.76 dB which is further improved to 6.26 dB, using the metamaterial surface. The radiation efficiency of the proposed metamaterial-based 5G antenna is above 85% at the desired central frequency.

Keywords: Metamaterial surface, in-phase reflection, 5G, high gain.

1 Introduction

Metamaterials are the periodic structures with properties, such as negative permeability, negative refractive index and double negative characteristic, etc., which do not exist in the natural materials [Alam, Misran, Yatim et al. (2013)]. The metamaterial antennas have become a great research hotspot [Faruque, Islam and Misran (2012)] due to their

[1] Department of Electrical Engineering, City University of Science and Information Technology, Peshawar, 25000, Pakistan.

[2] Faculty of Electrical Engineering, Ghulam Ishaq Khan Institute of Engineering Sciences and Technology, Topi, 23640, Pakistan.

[3] Department of Mechatronics Engineering, University of Engineering and Technology, Peshawar, 25000, Pakistan.

[4] School of Electrical Engineering, University of Ulsan, Ulsan, 44610, Korea.

[*] Corresponding Author: Sunghwan Kim. Email: sungkim@ulsan.ac.kr.

Received: 16 April 2020; Accepted: 08 May 2020.

unique properties, such as enhanced gain, efficiency and directivity etc., [Khan, Sehrai, Khan et al. (2019)]. The conventional ground plane does not offer enough surface waves suppression and in-phase reflection [Pepino, Mota, Martins et al. (2018)]; resulting in a side and back lobe which further affect the antenna performance such that, the gain of an antenna is lowered. However, incorporating a metamaterial surface with an antenna can improve its gain by providing the in-phase reflection to electromagnetic waves which radiates toward the backside of an antenna, causing the back lobes and degrading the gain of an antenna.

The lower portion of the spectrum is already highly congested by various technologies such as Bluetooth, wireless fidelity (Wi-Fi) and mobile communication, etc., while a large proportion of the centimeter wave spectrum, ranging from 3-300 GHz [Pi and Khan (2011); Khan, Sehrai and Ali (2019); Liu, Min, Ota et al. (2018); Li, Li, Shi et al. (2019)] is still unused and can be utilized for 5G communication system applications. The shifting towards the higher frequencies of the spectrum reduces the interference as well as helps to achieve the higher data rates [Li, Sim, Luo et al. (2017); Zhang, Ge, Li et al. (2017)] which is one of the most significant requirements of 5G systems. However, one of the main constrains which affects the antenna performance as we move ahead in the spectrum towards the higher frequencies is the atmospheric attenuations [Haraz, Elboushi, Alshebeili et al. (2014)] as compared to the lower frequencies of the centimeter wave spectrum [Sulyman, Alwarafy, MacCartney et al. (2016)]. The antenna with a high gain can help to overcome the atmospheric attenuations [Khan, Sehrai and Khan (2018); Khalid, Naqvi, Hussain et al. (2020); An, Li, Fu et al. (2018)]. Considering the fact, this works targets the frequency range from 3.3-3.6 GHz; the most obvious frequency band for 5G communication system applications [Wang, Qu, Wang et al. (2020); Abdullah, Kiani and Iqbal (2019); Abdullah, Kiani, Abdulrazak et al. (2019)], while the improved gain of the antenna further helps to reduce the path loss [Jiang, Si, Hu et al. (2019)] which occurs by progressing ahead in the frequency spectrum [Mak, Lai and Luk (2018); Dahri, Jamaluddin, Abbasi et al. (2017)] and improves the signal quality at the user end [Muhammad, Haroon, Abbas et al. (2019); Haroon, Abbas, Abbas et al. (2020); Haroon, Muhammad, Abbas et al. (2020); He, Xie, Xie et al. (2019)].

In literature, new methods for improving the gain of an antenna by utilizing the high impedance surface (HIS) characteristic of metamaterials are proposed. Jeong et al. [Jeong, Kim, Tentzeris et al. (2020)] have presented a monopole antenna operating at a central frequency of 2.7 GHz with a peak gain of 3.71 dB, incorporated with a metamaterial absorber. The improvement in gain is obtained up to 6.46 dB using a metamaterial absorber. The metamaterial medium is incorporated with a dipole antenna operating at a frequency of 60 GHz [Zarghooni, Dadgarpour and Denidni (2016)]; the gain enhancement achieved up to 2.4 dB. Liu et al. [Liu, Wang and Zeng (2013)] have proposed a microstrip antenna with a resonance frequency of 5.2 GHz using a negative permeability metamaterial. It attains a gain enhancement up to 1.5 dB. Han et al. [Han, Song and Sheng (2017)] have used an electromagnetic band gap (EBG) surface to improve the gain of a patch antenna by 2.5 dB; operating within a frequency range of 3.16 GHz to 3.36 GHz. A millimeter wave antenna (operating at a 60 GHz frequency band) employing different metamaterial surfaces is presented [Ullah, Ullah and Khan (2016)]. It achieves a maximum gain enhancement between the range of 0.65 to 1.6 dB, using a different metamaterial surface. However, the proposed metamaterial-based antennas achieve either less improvement in gain and are complex in structure. Khan et al. [Khan, Sehrai and Ahmad (2018)] have presented the simulated model of the 5G antenna. However, the gain achieves by their model at the lower band is not enough for the 5G systems as well as the radiation of an antenna is observed towards the backside of radiating element which is not desirable. Thus, these factors are considered in this paper and improved by using a novel design employing a metamaterial surface. Moreover, the proposed metamaterial-based antenna covers the most prominent frequency band of 5G, ranging from 3.3 GHz to 3.6 GHz.

1.1 Contributions

The main contributions of this paper can be summarized as follows:

1) In this paper, a high gain metamaterial based 5G antenna is presented, whereas the metamaterial surface is used as a reflector to improve the gain of an antenna by 3.5 dB.
2) The proposed metamaterial-based antenna covers the most prominent frequency band of 5G, ranging from 3.3 GHz to 3.6 GHz.
3) The antenna element is fabricated and tested to validate the simulated results.

1.2 Paper organization

The layout of the remaining paper is as follows. The geometry of the proposed 5G antenna and its design evaluation steps are discussed in Section II. Moreover, the detailed discussion on the designing of a unit cell followed by the analysis of its response is also presented in this section. The antenna is incorporated with the proposed metamaterial surface and its performance is analyzed in Section III. The results and discussion are also presented in this section. Section IV concludes the paper.

2 Geometry and design procedure

In this section, we present the geometry and design evaluation steps of the reference antenna (Fig. 1) and metamaterial unit cell (Fig. 3), which are designed in the Computer Simulation Technology (CST) Microwave Studio; a commercial electromagnetic software.

2.1 Antenna design

The geometry of the proposed antenna design is illustrated in Fig. 1. Rogers-4003 substrate with a size of $L \times W$= 44×39 mm^2 and a relative permittivity (ε_r), tangent loss of 3.55 and 0.0027, respectively is used in the design of the antenna. The substrate is backed by a trimmed ground plane. The total volume of the antenna is 44×39×1.524 mm^3. The various dimensions of the antenna as depicted in Fig. 1, are listed in Tab. 1. These dimensions are calculated in terms of guided wavelength ($\lambda_{3.6}$), using the Eqs. (1)-(3) [Balanis (2006)], for the desired operating frequency:

$$L_{3.6} = {}^{\lambda_{3.6}}/_{4} \tag{1}$$

$$\lambda_{fr} = \frac{c}{f_r\sqrt{\varepsilon_{eff}}} \text{ (GHz)} \tag{2}$$

$$\varepsilon_{eff} = \frac{\varepsilon_r+1}{2} + \frac{\varepsilon_r-1}{2}\left[1+12\frac{h}{W}\right]^{-\frac{1}{2}} \quad (3)$$

where λ_{fr} is the guided wavelength, fr is the resonant frequency, c is the velocity of light, W is the width of radiating element, ε_{eff} is the effective permittivity, and h is the substrate thickness.

Table 1: Summary of the dimensions of 5G antenna

Parameter	Value (mm)	Parameter	Value (mm)
y	44	h	1.1
x	39	g	8.0
n	18	f	2.0
m	44	e	4.5
l	4.0	d	5.0
k	3.4	c	5.0
j	3.0	b	31.5
i	0.1	a	3.0

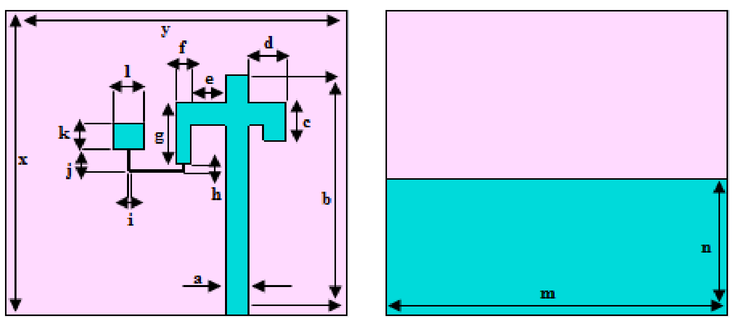

(a) (b)

Figure 1: Geometry of antenna (a) Front view (b) Back view

The radiating element (Fig. 1) is made by a process, depicted in Fig. 2(a). To obtain the resonance at the desired frequency band (3.6 GHz), the dimension of the strips and small patch within the radiating element of the proposed design are carefully chosen after a two-step design evaluation procedure as portrayed in Fig. 2(a). The return loss of the design steps is compared in Fig. 2(b). In Step 1, no modification in the radiating element does not give the satisfactory -10 dB bandwidth at the desired frequency; however, the consecutive improvements in return loss and -10 dB bandwidth are observed in Step 2. This modification in the radiating element illustrates that it is strongly responsible for the antenna to resonate at the desired 3.6 GHz frequency band with a satisfactory bandwidth.

2.2 Metamaterial surface design

Fig. 3, illustrates the geometry of the proposed unit cell. It is designed on a Rogers-4003 dielectric substrate with a dielectric constant 3.35, loss tangent 0.0027 and thickness 1.542 mm; backed by a finite ground plane. The response of the metamaterial surface depends on its unit cell. The proposed unit cell at two different design stages and their respective simulated reflection coefficient and in-phase reflection responses are shown in Fig. 4. As the unit cell designed in stage-1 (Fig. 4(a)), does not give a proper in-phase reflection

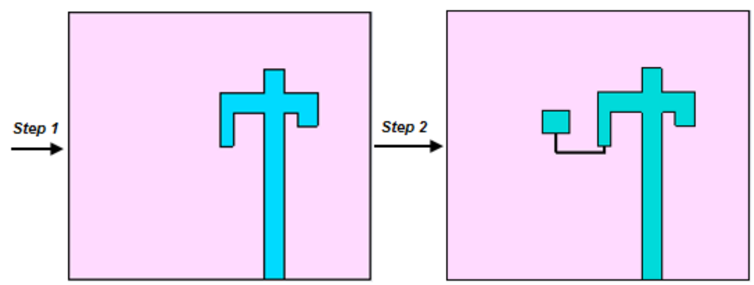

(a)

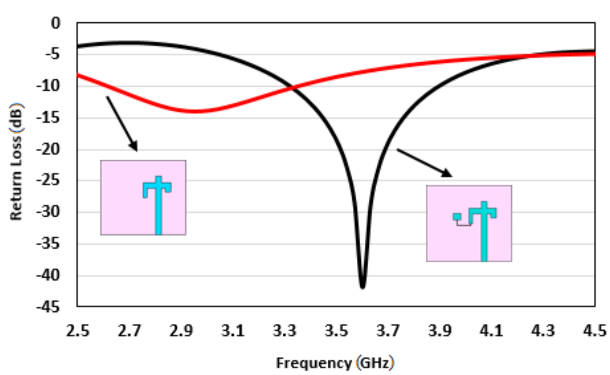

(b)

Figure 2: Design layout and return loss comparison (a) Design evaluation steps (b) Return loss comparison of the design evaluation steps

response (Fig. 4(c)) and reflection coefficient (Fig. 4(b)) at the desired frequency band due to the poor impedance matching. Therefore, strips are added at stage-2 (Fig. 4(a)), to improve the response of the proposed unit cell. A good impedance matching is observed at the desired frequency band; the reflection coefficient and in-phase reflection response are tuned at 3.6 GHz frequency band by the addition of strips. The resonant frequency of the unit cell can be adjusted by optimizing two variables, i.e., effective capacitance and inductance (*C and L*). The following equations [Bashir (2009); Iqbal, Saraereh, Bouazizi et al. (2018)] are used to control these parameters:

$$L = \mu_o h \quad (4)$$

$$C = \frac{w\varepsilon_0(1+\varepsilon_r)}{\pi} \cosh^{-1}\frac{a}{g} \quad (5)$$

$$f_r = \frac{1}{2\pi\sqrt{LC}} \tag{6}$$

where μ_o describes the free space permeability, g represents the gap between adjacent unit cells, w means the width of unit cell, and ε_o represents the permittivity of vacuum. Tab. 2, illustrates the parameters of the unit cell, given in Fig. 3.

Table 2: Parameters of the unit cell

Parameter	Value (mm)	Parameter	Value (mm)
p	10.0	wi	0.11
w1	0.21	r	0.22
o	0.21	q	2.50

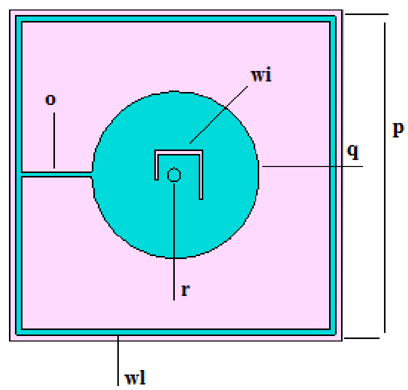

Figure 3: The proposed unit cell layout

3 5G antenna with metamaterial surface

To check the gain enhancement capability of the proposed metamaterial surface at the desired frequency band, a simple 5G antenna (as shown in Fig. 1) is placed ahead of the metamaterial surface. Fig. 5(a), shows the configuration of the proposed metamaterial surface. A 4×4 array of 16 elements is assembled by the replication of unit cells. The metamaterial surface is located below the antenna (Fig. 5(b)); thus, it can reflect the radiations of an antenna coming in the backward direction. If the reflected waves by the metamaterial surface are in phase at the antenna plane with the antenna's directly radiated waves, then the gain of antenna is increased. The altitude between the antenna and the metamaterial surface is an important factor to ensure the constructive interference of the reflected waves with the antenna's directly radiated waves. The following standard equation [Tahir, Arshad, Ullah et al. (2017)] is used to approximate the height.

$$\varphi - 2\beta H = 2n\pi;\ n=\ldots\text{-}1, 0, 1\ldots \tag{7}$$

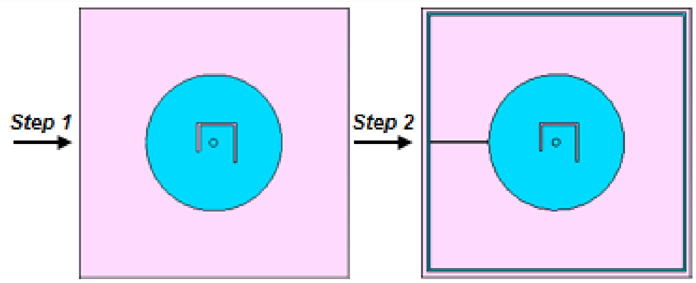

(a)

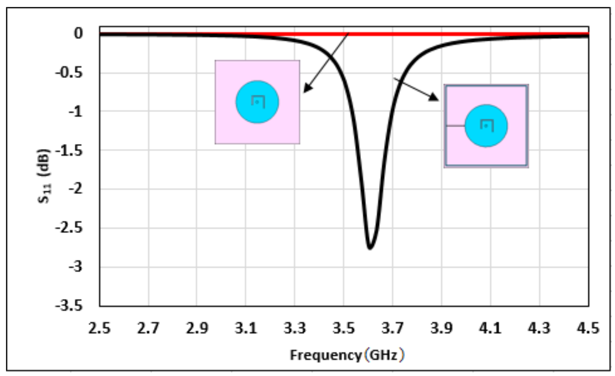

(b)

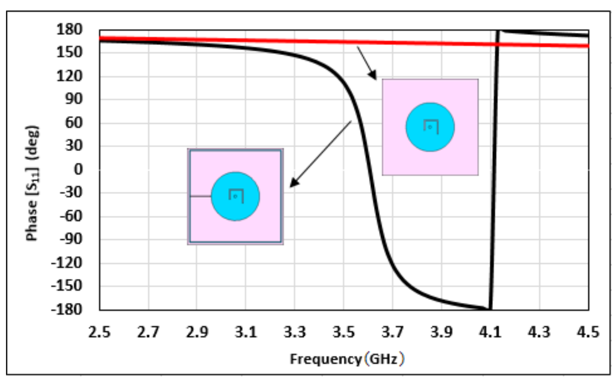

(c)

Figure 4: Unit cell (a) Design evaluation steps (b) Reflection coefficient comparison of these steps (c) In-phase reflection response comparison of these steps

Here H is the distance between the metamaterial surface and antenna, φ represents the reflection phase introduce by the metamaterial surface, and β is the free space propagation constant. Thus, the value of distance between the metamaterial surface and antenna, i.e., 0.4 λ_0 is chosen by using Eq. (7), where λ_0 is the free space wavelength.

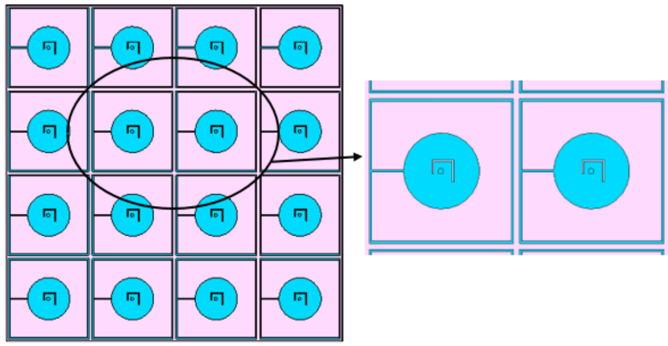

(a)

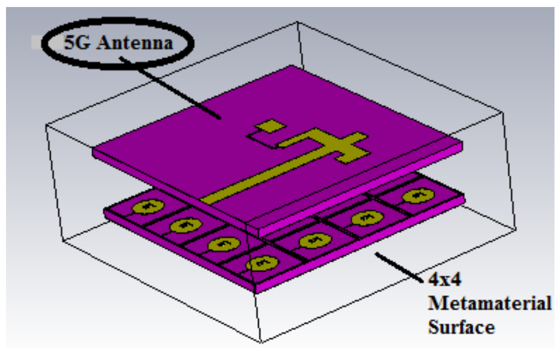

(b)

Figure 5: (a) 4×4 metamaterial surface (b) Antenna incorporated with a meta-surface

Fig. 6(a), depicts the computed return loss comparison of the antenna incorporating a metamaterial surface and without the reflector. The return loss is lower than -10 dB for the desired frequency band; antenna without a metamaterial surface has a minimum return loss of -42.0 dB at 3.60 GHz central frequency, and the antenna with a metamaterial surface possesses a return loss of -32 dB at 3.32 GHz frequency. This deviation in frequency is due to the change in current on the surface of the antenna; triggered by the reflections from the metamaterial surface. To support the return loss comparison of the proposed antennas, the voltage standing wave ratio (VSWR) comparison is also analyzed (Fig. 6(b)). The antenna with and without metamaterial surface gives VSWRs of 1.05 and 1.01, respectively, with an input impedance of nearly 50 Ω. It is evident from Fig. 6b that the antenna is properly matched with a VSWR<1.1 for the two cases.

The 2D radiation patterns (Fig. 7) of the antenna with and without metamaterial surface at the desired frequency band are shown in the two principal planes, i.e., E-Plane (XZ, $\phi=0^0$) and H-plane (YZ, $\phi=90^0$). The gain of the antenna without a metamaterial surface is observed 2.76 dB, while after incorporating a metamaterial surface as a reflector, it yields a highest gain of 6.26 dB with a radiation efficiency of above 85% in both cases.

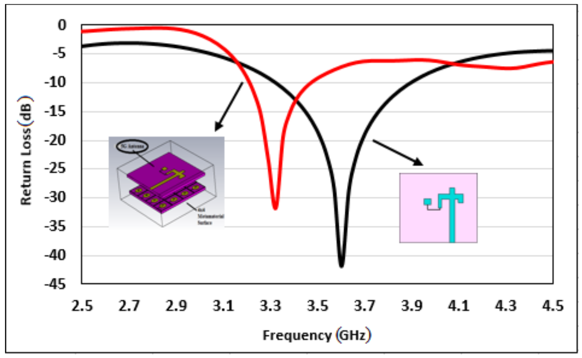

(a)

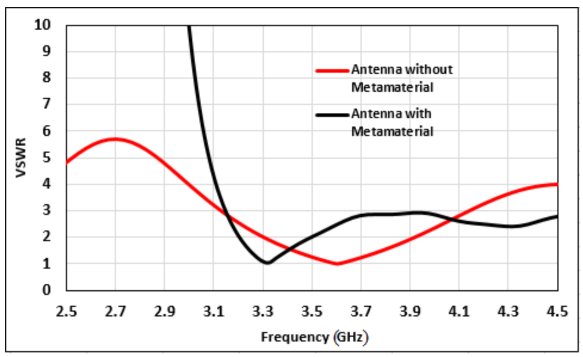

(b)

Figure 6: Antenna with and without metamaterial surface (a) Return loss comparison (b) VSWR comparison

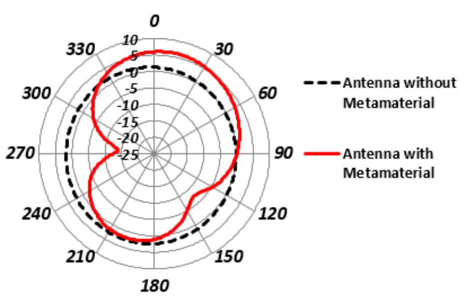

(a)

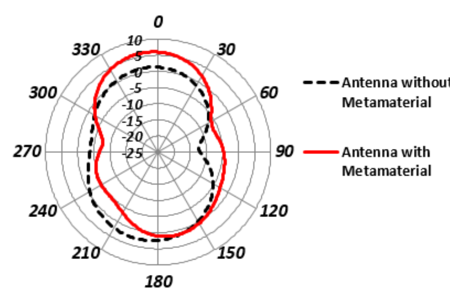

(b)

Figure 7: Radiation pattern (2D) (a) E plane (b) H plane

Moreover, the metamaterial-based antenna shows a 3 dB beamwidth and main lobe direction of 91.6°, 10.0° and 64.2°, 6.0° in the E and H planes, respectively. The side lobe levels of -4.2 dB and -4.7 dB is obtained in the corresponding planes (E and H, respectively). For further clarification the snapshot of the surface current density of an antenna with and without metamaterial surface is shown in Fig. 8. It is observed that the overall effective resonant length of the antenna is responsible for radiation.

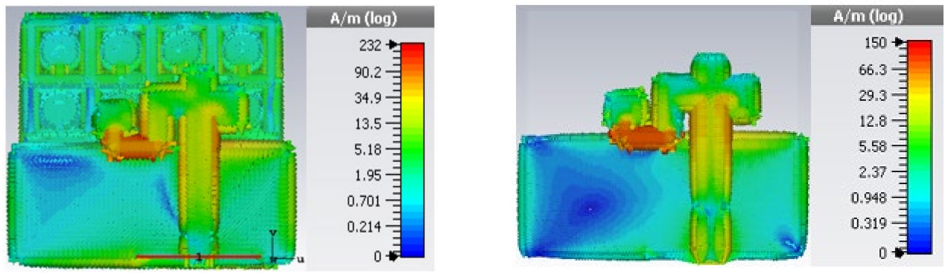

(a) (b)

Figure 8: Surface current distribution (a) Metamaterial-based antenna (b) Antenna without metamaterial surface

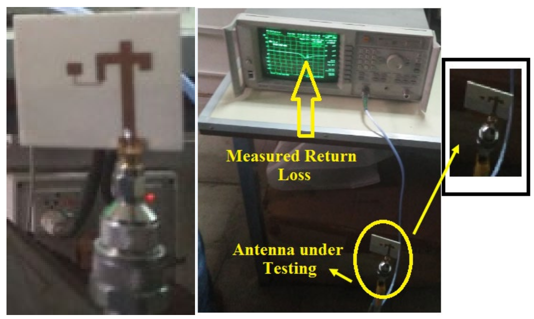

(a) (b)

Figure 9: Fabricated antenna (a) Connected with a connector (b) Under testing

The proposed 5G antenna is fabricated on a Rogers-4003 substrate (Fig. 9(a)) and the return loss of an antenna is measured (Fig. 9(b)). The 2D radiation pattern (Fig. 10) in the two principle planes, i.e., H and E planes, of the antenna are measured using the anechoic chamber far-field measurement system. We observe a good coherence in the simulated and measured results.

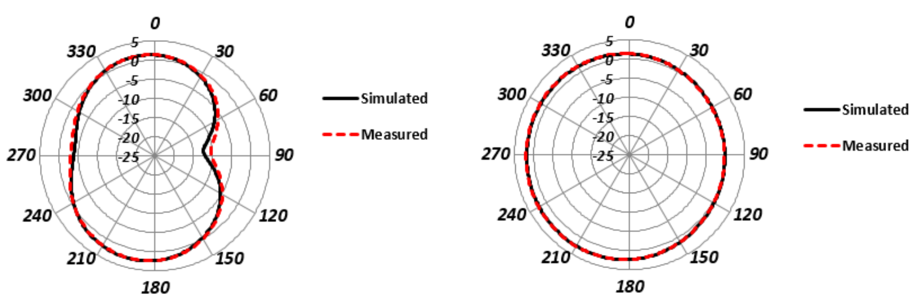

(a) (b)

Figure 10: Simulated and measured results (a) H-plane (b) E-plane

4 Conclusion

In this work, the analysis of an antenna incorporating a metamaterial surface operating in the most prominent 5G frequency band (3.3-3.6 GHz) is proposed. Rogers-4003 is used as substrate in the design of the antenna with and without metamaterial surface. The gain of a reference antenna is 2.76 dB, operating at a 3.6 GHz frequency band which is further improved up to 6.26 dB by using a metamaterial surface as a reflector. The average improvement in gain of 3.5 dB is observed. The metamaterial surface acts as a high impedance surface which reflects the antenna's back side radiations to achieve the improvement in the gain. Therefore, the proposed metamaterial-based antenna can be used for 5G communication system applications. The reference antenna is experimentally demonstrated and a good coherence in the simulated and the measured results is achieved. Our keen interest in the future will be to fabricate the prototype of metamaterial surface and its results validation.

Funding Statement: This work was supported by the Research Program through the National Research Foundation of Korea, NRF-2019R1A2C1005920, S. K.

Conflicts of Interest: The authors declare that they have no conflicts of interest to report regarding the present study.

References

Abdullah, M.; Kiani, S. H.; Abdulrazak, L. F.; Iqbal, A.; Bashir, M. A. et al. (2019): High-performance multiple-input multiple-output antenna system for 5G mobile terminals. *Electronics*, vol. 8, pp. 1090.

Abdullah, M.; Kiani, S. H.; Iqbal, A. (2019): Eight element multiple input multiple output (MIMO) antenna for 5G mobile applications. *IEEE Access*, vol. 7, pp. 134488-134495.

Alam, Md. S.; Misran, N.; Yatim, B.; Islam, M. T. (2013): Development of electromagnetic band gap structures in the perspective of microstrip antenna design. *Journal of Antennas and Propagation*, vol. 2013.

An, W.; Li, Y.; Fu, H.; Ma, J.; Chen, W. et al. (2018): Low-profile and wideband microstrip antenna with stable gain for 5G wireless applications. *IEEE Antennas and Wireless Propagation Letters*, vol. 17, no. 4, pp. 621-624.

Balanis, C. A. (2006): Antenna theory: analysis and design. *John Wiley and Sons*.

Bashir, S. (2009): Design and synthesis of non-uniform high impedance surface based wearable antennas. *PhD. Dissertation, Department of Electronics and Electrical Engineering*, Loughborough University, Leicestershire, United Kingdom.

Dahri, M. H.; Jamaluddin, M. H.; Abbasi, M. I.; Kamarudin, M. R. (2017): A review of wideband reflect array antennas for 5G communication systems. *IEEE Access*, vol. 5, pp. 17803-17815.

Faruque, M. R. I.; Islam, M. T.; Misran, N. (2012): Design analysis of new metamaterial for EM absorption reduction. *Progress in Electromagnetics Research*, vol. 124, pp. 119-135.

Han, Z.; Song, W.; Sheng, X. (2017): Gain enhancement and RCS reduction for patch antenna by using polarization-dependent EBG surface. *IEEE Antennas and Wireless Propagation Letters*, vol. 16, pp. 1631-1634.

Haraz, O. M.; Elboushi, A.; Alshebeili, S. A.; Sebak, A. (2014): Dense dielectric patch array antenna with improved radiation characteristics using EBG ground structure and dielectric superstrate for future 5G cellular networks. *IEEE Access*, vol. 2, pp. 909-913.

Haroon, M. S.; Abbas, Z. H.; Abbas, G.; Muhammad, F. (2020): SIR analysis for non-uniform HetNets with joint decoupled association and interference management. *Computer Communications*, vol. 155, pp. 48-57.

Haroon, M. S.; Muhammad, F.; Abbas, Z. H.; Abbas, G. (2020): Proactive uplink interference management for nonuniform heterogeneous cellular networks. *IEEE Access*, vol. 8, no. 1, pp. 55501-55512.

He, S. M.; Xie, K.; Xie, K. X.; Xu, C.; Wang, J. (2019): Interference-aware multisource transmission in multiradio and multichannel wireless network. *IEEE Systems Journal*, vol. 13, no. 3, pp. 2507-2518.

Iqbal, A.; Saraereh, O. A.; Bouazizi, A.; Basir, A. (2018): Metamaterial-based highly isolated MIMO antenna for portable wireless applications. *Electronics*, vol. 7, no. 10, pp. 267.

Jeong, H.; Kim, Y.; Tentzeris, M. M.; Lim, S. (2020): Gain-enhanced metamaterial absorber-loaded monopole antenna for reduced radar cross-section and back radiation. *Materials*, vol. 13, no. 5, pp. 1247.

Jiang, H.; Si, L. M.; Hu, W.; Lv, X. (2019): A symmetrical dual-beam bowtie antenna with gain enhancement using metamaterial for 5G MIMO applications. *IEEE Photonics Journal*, vol. 11, no. 1, pp. 1-9.

Khalid, M.; Naqvi, S. I.; Hussain, N.; Rahman, M.; Fawad et al. (2020): 4-port MIMO antenna with defected ground structure for 5G millimeter wave applications. *Electronics*, vol. 9, pp. 71.

Khan, J.; Sehrai, D. A.; Ahmad, S. (2018): Design and performance comparison of metamaterial-based antenna for 4G/5G mobile devices. *World Academy of Science, Engineering and Technology, International Science Index 138, International Journal of Electronics and Communication Engineering*, vol. 12, no. 6, pp. 382-387.

Khan, J.; Sehrai, D. A.; Ali, U. (2019): Design of dual band 5G antenna array with SAR analysis for future mobile handsets. *Journal of Electrical Engineering & Technology*, vol. 14, no. 2, pp. 809-816.

Khan, J.; Sehrai, D. A.; Khan, M. A.; Khan, H. A.; Ahmad, S. et al. (2019): Design and performance comparison of rotated Y-shaped antenna using different metamaterial surfaces for 5G mobile devices. *Computers, Materials & Continua*, vol. 60, no. 2, pp. 409-420.

Khan, J.; Sehrai, D. A.; Khan, S. (2018): Next generation mobile phone antenna and its SAR investigation. *Sindh University Research Journal-SURJ (Science Series)*, vol. 50, no. 1, pp. 27-32.

Li, Y.; Li, J.; Shi, P.; Qin X. (2019): Building an open cloud virtual dataspace model for materials scientific data. *Intelligent Automation and Soft Computing*, vol. 25, no. 3, pp. 615-624.

Li, Y.; Sim, C. Y. D.; Luo, Y.; Yang, G. (2017): 12-Port 5G massive MIMO antenna array in sub-6GHz mobile handset for LTE bands 42/43/46 applications. *IEEE Access*, vol. 6, pp. 344-354.

Liu, A. F.; Min, J.; Ota, K.; Zhao, M. (2018): Reliable differentiated services optimization for network coding cooperative communication system. *Computer Systems Science and Engineering*, vol. 33, no. 4, pp. 235-250.

Liu, Z.; Wang, P.; Zeng, Z. (2013): Enhancement of the gain for microstrip antennas using negative permeability metamaterial on low temperature co-fired ceramic (LTCC) substrate. *IEEE Antennas and Wireless Propagation Letters*, vol. 12, pp. 429-432.

Mak, K. M.; Lai, H. W.; Luk, K. M. (2018): A 5G wideband patch antenna with antisymmetric L-shaped probe feeds. *IEEE Transactions on Antennas and Propagation*, vol. 66, no. 2, pp. 957-961.

Muhammad, **F.; Haroon, M. S.; Abbas, Z. H.; Abbas, G.; Kim, S.** (2019): Uplink interference management for HetNets stressed by clustered wide-band jammers. *IEEE Access*, vol. 7, no. 1, pp. 182679-182690.

Pepino, V. M.; Mota, A. F. da.; Martins, A.; Borges, B. H. V. (2018): 3D-printed dielectric metasurfaces for antenna gain improvement in the Ka-band. *IEEE Antennas and Wireless Propagation Letters*, vol. 17, no. 11, pp. 2133-2136.

Pi, Z.; Khan, F. (2011): An introduction to millimeter-wave mobile broadband systems. *IEEE Communications Magazine*, vol. 49, no. 6, pp. 101-107.

Sulyman, A. I.; Alwarafy, A.; MacCartney, Jr., G. R.; Rappaport, T. S.; Alsanie, A. (2016): Directional radio propagation path loss models for millimeter-wave wireless networks in the 28, 60, and 73 GHz bands. *IEEE Transactions on Wireless Communications*, vol. 15, no. 10, pp. 6939-6947.

Tahir, F. A.; Arshad, T.; Ullah, S.; Flint, J. A. (2017): A novel FSS for gain enhancement of printed antennas in UWB frequency spectrum. *Microwave and Optical Technology Letters*, vol. 59, pp. 2698-2704.

Ullah, S.; Ullah, S.; Khan, S. (2016): Design and analysis of a 60 GHz millimeter wave antenna. *Jurnal Teknologi*, vol. 78, no. 3, pp. 63-68.

Wang, H.; Qu, S.; Wang, J.; Yan, M.; Zheng, L. (2020): Dual-band miniaturised FSS with stable resonance frequencies of 3.4/4.9 GHz for 5G communication systems applications. *IET Microwaves, Antennas & Propagation*, vol. 14, no. 1, pp. 1-6.

Zarghooni, B.; Dadgarpour, A.; Denidni, T. A. (2016): Millimeter-wave antenna using two-sectioned metamaterial medium. *IEEE Antennas and Wireless Propagation Letters*, vol. 15, pp. 960-963.

Zhang, J.; Ge, X.; Li, Q.; Guizani, M.; Zhang, Y. (2017): 5G millimeter-wave antenna array: design and challenges. *IEEE Wireless Communications*, vol. 24, pp. 106-112.